The Astrophysical Journal, 675:L97–L100, 2008 March 10

GEOMETRY DIAGNOSTICS OF A STELLAR FLARE FROM FLUORESCENT X-RAYS

Paola Testa,[1] Jeremy J. Drake,[2] Barbara Ercolano,[2] Fabio Reale,[3,4] David P. Huenemoerder,[1] Laura Affer,[3,4] Giuseppina Micela,[4] and David Garcia-Alvarez[2,5]

Received 2007 September 25; accepted 2008 January 23; published 2008 February 19

ABSTRACT

We present evidence of Fe fluorescent emission in the *Chandra* HETGS spectrum of the single G-type giant HR 9024 during a large flare. In analogy to solar X-ray observations, we interpret the observed Fe Kα line as being produced by illumination of the photosphere by ionizing coronal X-rays, in which case, for a given Fe photospheric abundance, its intensity depends on the height of the X-ray source. The HETGS observations, together with three-dimensional Monte Carlo calculations to model the fluorescence emission, are used to obtain a direct geometric constraint on the scale height of the flaring coronal plasma. We compute the Fe fluorescent emission induced by the emission of a single flaring coronal loop that well reproduces the observed X-ray temporal and spectral properties according to a detailed hydrodynamic modeling. The predicted Fe fluorescent emission is in good agreement with the observed value within observational uncertainties, pointing to a scale height $\lesssim 0.3R_*$. Comparison of the HR 9024 flare with that recently observed on II Peg by *Swift* indicates the latter is consistent with excitation by X-ray photoionization.

Subject headings: hydrodynamics — plasmas — stars: coronae — X-rays: stars

1. INTRODUCTION

Since the early 1970s, spatially resolved observations of the solar corona have revealed a high degree of structuring over all scales, from of order the solar radius down to instrumental resolution limits (e.g., Vaiana et al. 1973a, 1973b). This spatial structuring is intimately linked to the characteristics of magnetic field generation and interaction and to plasma heating mechanisms. On other stars, especially very active ones (with X-ray luminosity L_X up to $10^4 \times L_{X\odot}$), coronal structure and its relation with stellar parameters such as mass, rotation, and evolutionary phase remains very uncertain.

Techniques used to date to investigate the morphology of stellar coronae comprise rotational modulation (e.g., Marino et al. 2003; Flaccomio et al. 2005), flare modeling (e.g., Reale et al. 2004; Testa et al. 2007b, hereafter Paper I), eclipse mapping (e.g., White et al. 1990), spectroscopic density and radiation field diagnostics (e.g., Testa et al. 2004a; Ness et al. 2004), resonance scattering (e.g., Testa et al. 2004b; Matranga et al. 2005; Testa et al. 2007a), velocity modulation (e.g., Brickhouse et al. 2001; Chung et al. 2004; Hussain et al. 2005; Huenemoerder et al. 2006), and simultaneous Doppler imaging and X-ray spectroscopy (Hussain et al. 2007).

The fluorescent iron line at ~6.4 keV[6] presents a further, potentially powerful diagnostic of stellar coronal geometry. Extensively used in study of active galactic nuclei and X-ray binaries (see, e.g., reviews by George & Fabian 1991; Reynolds & Nowak 2003) and often seen on the Sun during flares (Culhane et al. 1981; Parmar et al. 1984; Tanaka et al. 1984; Zarro et al. 1992; Phillips et al. 1994), the line is produced by electron cascade after one of the two K-shell ($n = 1$) electrons of an iron atom (or ion) is ejected following photoelectric absorption of X-rays. In the solar and stellar case, for a given irradiating flare spectrum, the line strength depends essentially on three parameters: flare height, heliocentric angle, and photospheric Fe abundance (e.g., Bai 1979; Drake et al. 2007b, hereafter D07b). If it can be observed in stars, Fe K fluorescence therefore presents a means of estimating flare and coronal scale height.

Fe fluorescence has now been detected on a number of pre–main-sequence (PMS) stars with disks (e.g., Tsujimoto et al. 2005; Favata et al. 2005), where it is most likely produced by coronal X-ray irradiation of the cold disk material. Here we present evidence for *photospheric* Fe fluorescent emission in the *Chandra* HETGS spectrum of the X-ray–active single G1 giant HR 9024 (see Paper I and references therein for a description of the characteristics of the target). The observations and analysis are briefly described in § 2. In § 3 we present three-dimensional (3D) Monte Carlo calculations of the Fe Kα fluorescence. The results are presented in § 4, where we derive an estimate for the coronal scale height and compare it with the prediction of the loop hydrodynamic model that succeeds in describing the observed flaring spectrum (Paper I). To our knowledge, the HR 9024 *Chandra* spectrum represents only the second detection of Fe photospheric fluorescence. Very recently, the line was observed by the *Swift* X-Ray Telescope during a "superflare" on the RS CVn binary system II Peg by Osten et al. (2007), who ascribed the excitation mechanism to electron impact ionization of photospheric Fe instead of photoionization. We discuss our result and the II Peg observations in § 5 and show that the latter is also consistent with, and more plausibly associated with, photoionization than electron impact.

2. OBSERVATIONS AND DATA ANALYSIS

Chandra High Energy Transmission Grating (Canizares et al. 2005) observations of HR 9024 (ObsID 1892) were discussed in detail by Paper I, which analyzed the X-ray spectra and variability of HR 9024 and constructed a flaring loop hy-

[1] Massachusetts Institute of Technology, Kavli Institute for Astrophysics and Space Research, 70 Vassar Street, Cambridge, MA 02139; testa@space.mit.edu.

[2] Smithsonian Astrophysical Observatory, MS 3, 60 Garden Street, Cambridge, MA 02138.

[3] Dipartimento di Scienze Fisiche e Astronomiche, Università di Palermo Piazza del Parlamento 1, 90134 Palermo, Italy.

[4] INAF-Osservatorio Astronomico di Palermo, Piazza del Parlamento 1, 90134 Palermo, Italy.

[5] Imperial College London, Blackett Laboratory, Prince Consort Road, London SW7 2AZ, UK.

[6] The Fe fluorescent feature actually consists of two components, at 6.391 and 6.404 keV (for Fe I), which are unresolved by present instruments; therefore, hereafter we will refer to the feature as a single emission line.

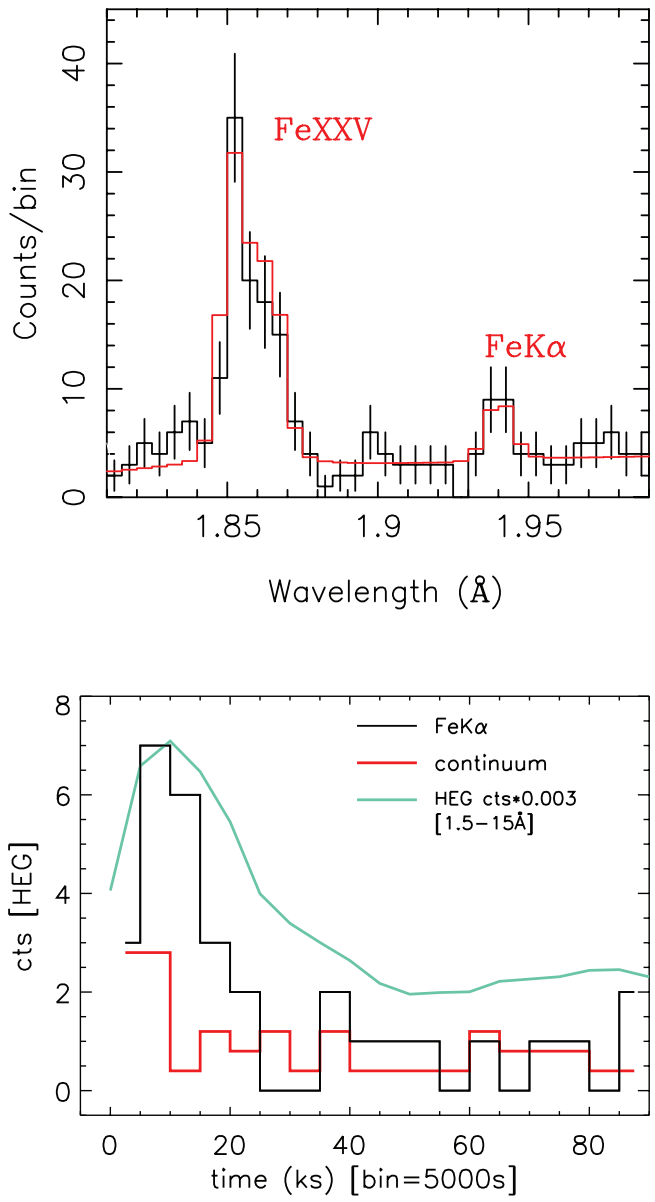

FIG. 1.—*Top:* HEG spectrum of HR 9024 during the flare (first 40 ks of the observation) in the wavelength range containing the Fe XXV coronal emission (~1.85 Å) and the Fe Kα emission (~1.94 Å), with the best-fit model. *Bottom:* Comparison of light curve of the Kα emission (*black*) with the adjacent continuum background emission (*red*); the continuum is extracted on a wavelength region (1.912–1.932 Å+1.948–1.968 Å) that is 2.5 times larger than the wavelength extraction region used for the Fe Kα and then appropriately scaled. We also plot the scaled light curve of dispersed photons integrated in the HEG band (*green curve*). A temporal bin size of 5 ks is used for all light curves. We plot counts (scaled by 0.003 in the case of the integrated HEG band); therefore, the associated uncertainties correspond to the Poisson errors.

drodynamic model that successfully reproduced the observations. We analyze the same data here, using the PINTofALE[7] IDL[8] software (Kashyap & Drake 2000) and the Interactive Spectral Interpretation System (ISIS)[9] version 1.4.2 (Houck & Denicola 2000).

The HEG flare spectrum (first 40 ks of the observation) in the wavelength region with the Fe Kα emission is illustrated

[7] http://hea-www.harvard.edu/PINTofALE.
[8] Interactive Data Language, Research Systems, Inc.
[9] ISIS is available at http://space.mit.edu/cxc/isis/.

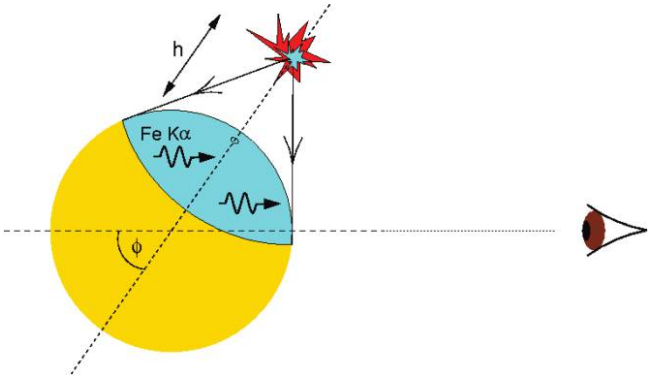

FIG. 2.—Geometry for fluorescent excitation of photospheric Fe Kα by coronal X-rays emitted by a source located at height h above the photosphere. ϕ is the angle of inclination with respect to the line of sight.

in Figure 1 (*top panel*), together with a comparison between the evolution of the fluorescent and adjacent continuum emission (*bottom panel*). A Kolmogorov-Smirnov test applied to the light curves of Fe Kα and the nearby continuum indicates that they are significantly different during the flare, $P < 10^{-10}$, but $P \sim 0.94$ during the rest of the observation. The Fe Kα line flux was measured with ISIS by convolving a Gaussian profile with the instrumental response, using the continuum predicted by an isothermal spectral model described in § 3 (and derived in Paper I). We obtained an Fe Kα line flux of 1.7×10^{-5} photons cm^{-2} s^{-1}, with a corresponding 90% confidence range (0.8–2.8) $\times 10^{-5}$ photons cm^{-2} s^{-1}.

3. FLUORESCENCE MODELING

The basic physics of Fe fluorescent line production on the Sun has been investigated through detailed Monte Carlo calculations of the interaction between a hard X-ray continuum ($E > 7.11$ keV) and dense, neutral photospheric material by Bai (1979), considering a thermal continuum and taking into account the curvature of the solar photosphere. The problem has been further discussed in detail in the stellar context by D07b.

We used a modified version of the 3D radiative transfer code MOCASSIN (Ercolano et al. 2003, 2007; Drake & Ercolano 2007) to carry out Monte Carlo calculations to follow the Fe Kα photons resulting from X-ray absorption and to determine the emerging Fe Kα emission as a function of the flare geometry parameters illustrated in Figure 2. Here, our method differs from the calculations of Bai (1979) in that we can use any given input fluorescing spectrum, whereas Bai (1979) adopted an analytical expression for the thermal bremsstrahlung continuum and computed a grid for T in the range 0.5–5 keV. Detailed descriptions of the methods used for the fluorescence calculations are presented by D07b.

We note that the fluorescence efficiency, $\mathcal{E}$, defined as the ratio of the Fe Kα flux to one-half the integral of the X-ray flux above 7.11 keV ($\mathcal{E} = I(\text{Fe K}\alpha)/[I_c(E > 7.11\ \text{keV})/2]$), is only very weakly dependent on the photospheric metallicity, [M/H] (D07b). For HR 9024 no accurate photospheric abundances were available, and we therefore obtained optical spectra with the high-resolution ($R = 86{,}000$) spectrograph SARG at the Telescopio Nazionale Galileo and derived a near-solar photospheric Fe abundance [Fe/H] $= -0.2 \pm 0.3$ (L. Affer et al., in preparation). On the basis of the calculations of D07b, we find an uncertainty in $\mathcal{E}$ of $\pm 25\%$ for a metallicity uncertainty range [M/H] $= -0.5$–$+0.1$, including allowance for an over-

abundance of α-elements with respect to Fe at the low-metallicity end of 0.2–0.3 dex (e.g., Bensby et al. 2003).

In order to compute $\mathcal{E}$, we used a fluorescing spectral model with $\log T[\mathrm{K}] = 7.8$, and $\log \mathrm{EM}[\mathrm{cm}^{-3}] = 54.9$, based on the values found from the analysis of the continuum emission in the early phases of the flare (see Fig. 6 of Paper I). This was preferred over a spectrum computed using the emission measure distribution, EM(T), derived for the flare as a whole (rise+peak+decay; see Figs. 3 and 6 of Paper I) because most of the Fe Kα emission is detected in the rise, peak, and early decay phases: the use of the whole flare EM(T) would slightly underestimate the hard X-ray flux. Values of $\mathcal{E}$ were calculated assuming a point source for the flare and for a range of flare heights, h. The results obtained for a range of flare heights and line-of-sight viewing angles are shown in Figure 3.

As expected, the model fluorescent efficiency declines strongly for larger values of h, the height of the flaring source. This occurs because of the $1/h^2$ dilution of the irradiating surface flux and because photon incidence angles become larger, causing the average depth where the photoionization takes place to increase. For the line-of-sight viewing angle $\phi \lesssim 60°$, the fluorescence efficiency depends primarily on h but not on ϕ; for $\phi > 60°$, the efficiency rapidly decreases.[10]

In Paper I we modeled the observed flare using a hydrodynamic treatment of the evolution of the flaring plasma within the confines of a single long loop. The hydrodynamic model provides us with the physical conditions (in particular, T and n_e) of each plasma volume element along the loop, allowing us to compute the expected Fe Kα emission for a direct comparison with the measured fluorescence efficiency. In order to calculate the $\mathcal{E}$ induced by the emission of the flaring loop as resulting from the hydrodynamic modeling, we proceeded as follows: (1) we synthesized hard X-ray spectra (7–50 keV) for isothermal plasmas for a grid of temperatures covering a large T range ($\log T = 5$, 8.5); (2) we divided the half-loop into four different segments and computed the hard X-ray spectrum of each segment by adding the spectra of all volume elements (each characterized by a temperature and emission measure) within the segment, integrating over the 40 ks of the flare; and (3) we computed the expected fluorescence emission induced by each segment, depending on its input spectrum and corresponding height, and computed the overall Fe Kα emission, and therefore the predicted $\mathcal{E}$. Splitting the loop into segments linearly spaced in h (i.e., $h_i = \{0.125, 0.375, 0.625, 0.875\} \times h$), assuming that the loop is perpendicular to the stellar surface, we obtain $\mathcal{E}(\mathrm{HD\ mod}) = 0.016$. We also computed the efficiency using a logarithmic spacing ($h_i = \{0.0065, 0.028, 0.118, 0.504\} \times h$), and we find $\mathcal{E}(\mathrm{HD\ mod}) = 0.018$, only slightly different from the former value.

4. RESULTS

To compare the observed Fe Kα flux with model values, we used the same spectral model based on the observed continuum described above. The one-half integrated X-ray flux above 7.11 keV (up to 50 keV) as computed from this model is 7.5×10^{-4} photons cm^{-2} s^{-1}, which, when combined with the observed Fe Kα flux, yields a value for the observed fluorescence efficiency $\mathcal{E} = 0.022$ [0.010–0.033]. We note that at 50 keV the flux is already several orders of magnitude lower than at 7.11 keV, therefore the efficiency does not depend significantly on this upper bound value used for the energy range. In Figure 3, the measured value, with the 90% confidence range, is represented as a shaded area superposed to the theoretical curves derived in § 3.

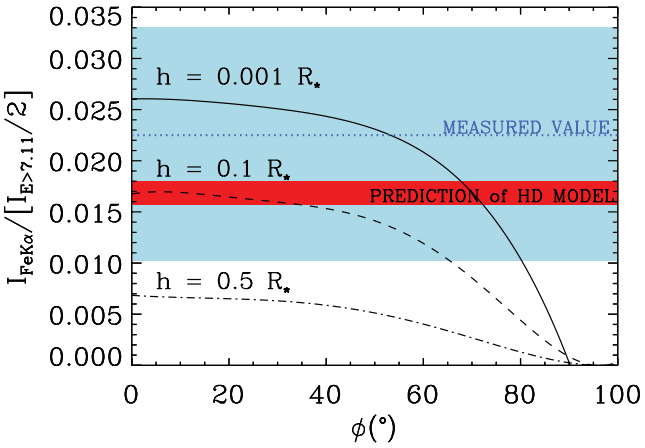

FIG. 3.—Theoretical curves of fluorescence efficiency (*black curves*), obtained using the MOCASSIN code, as a function of the angle of inclination with respect to the line of sight, ϕ, for different heights of the hard X-ray source: $h = 0.001R_*$, $0.1R_*$, and $0.5R_*$. We superpose the measured value (*blue dotted line*) with the corresponding 90% confidence range (*shaded light blue area*) and the prediction of the hydrodynamic loop model (*red shaded area*).

The comparison between observed and model values of $\mathcal{E}$ implies for the scale height an upper limit of $\sim 0.3R_*$, where $R_* = 13.6R_\odot$ (Singh et al. 1996). This result compares well with the hydrodynamic modeling that finds a loop semilength $L \sim 0.5R_*$ (Paper I), corresponding to a loop apex at $h = L \times 2/\pi = R_*/\pi \sim 0.32R_*$ (assuming that the loop is perpendicular to the stellar surface, otherwise $h < 0.32R_*$). The efficiency expected on the basis of the hydrodynamic model itself corresponds to an "effective scale height" $h \sim 0.1R_*$—somewhat lower that the maximum height of the loop model. This can be understood on the basis of the extreme characteristics of the flaring loop in HR 9024, which is much hotter than typical solar flares: for solar flares, typically reaching temperatures $\gtrsim 10^7$ K, the hard X-ray photons above the 7.11 keV threshold will be emitted almost uniquely by the hotter loop apex; instead, in the flaring loop on HR 9024, with peak temperature of the order of 10^8 K, the lower coronal plasma will still be effective in producing hard X-ray photons because of its elevated temperature (of several 10^7 K) and density.

5. DISCUSSION AND CONCLUSIONS

We have presented the first detailed analysis of observed photospheric fluorescence to probe the geometric properties of stellar coronal emission. For the flare on HR 9024 we find the observed Fe Kα intensity completely consistent with production through photospheric irradiation by flare X-rays. Our estimate for the flare scale height of $h \lesssim 0.3R_*$ provides a cross-check for the results of the hydrodynamic modeling of the flare observed on HR 9024 that can be satisfactorily reproduced by a single flaring loop of semilength $L = 0.5R_*$. The agreement between the observed $\mathcal{E}$ and the value computed directly from this model provides further confidence both in the hydrodynamic modeling approach and in X-ray fluorescence as the excitation mechanism for the Fe Kα line. We note that our model based on *Chandra* data might underestimate the high-energy continuum flux because we cannot detect any additional

[10] The results are qualitatively similar also for the case of the semi-infinite slab in George & Fabian (1991).

(either thermal or nonthermal) emission possibly present at energies outside the *Chandra* band. However, if additional high-energy emission were present, the higher flux above 7.11 keV would make the efficiency lower, bringing it in even better agreement with the predictions of the model.

As noted in § 1, Fe Kα emission has been extensively observed in solar X-ray spectra during flares (Culhane et al. 1981; Parmar et al. 1984; Tanaka et al. 1984; Zarro et al. 1992; Phillips et al. 1994). Two main production mechanisms were initially explored to explain the line: electron impact from a nonthermal electron population and X-ray photoionization. The observed Fe Kα evolution with respect to the thermal and nonthermal emission, and the observed center-to-limb variations seen on the Sun, strongly support the X-ray fluorescence mechanism (Culhane et al. 1981; Parmar et al. 1984; Tanaka et al. 1984), although in rare cases there is indication that electron impact might contribute during the early impulsive phase (e.g., Emslie et al. 1986). Ballantyne & Fabian (2003) have also shown that Fe K production in accretion disks by nonthermal electron bombardment is extremely unlikely and requires 2–4 orders of magnitude greater energy dissipation in the electron beam than is required for an X-ray photoionization source. In this context, the recent observations of an extremely large Fe Kα equivalent width in the PMS star V1486 Ori (Czesla & Schmitt 2007), and variability in Fe Kα emission uncorrelated with the observed X-ray continuum on Elias 29 (Giardino et al. 2007), seem to challenge the photoionization excitation mechanism. However, D07b note that fluorescence from PMS disks excited by X-rays originating from the unseen stellar hemisphere will also be observed: in $\lesssim$50% of cases, Fe Kα can then appear anomalous when compared only to the *observed* thermal continuum.

To date, the *Swift* observation of II Peg (Osten et al. 2007) is the only other case in which Fe Kα emission has been observed for a star (other than the Sun) lacking substantial circumstellar material. Osten et al. (2007) dismissed X-ray fluorescence as the excitation mechanism on the basis of arguments for fluorescence in an optically thin medium and instead attributed the Fe Kα to electron impact with nonthermal electrons. As noted in earlier discussions (e.g., Parmar et al. 1984; Ballantyne & Fabian 2003), one major problem for an electron impact excitation mechanism is the inefficiency of this process. Extremely large energies must be dissipated in accelerated electron beams to produce continuum and fluorescence emission that might be observed on a star. Indeed, Osten et al. (2007) showed that the hard X-ray continuum observed in the II Peg flare would require an energy of 3×10^{40} ergs in nonthermal electrons if interpreted in terms of thick-target bremsstrahlung. Over the time of the duration of the flare, this corresponds to an energy dissipation rate in accelerated electrons of more than 100 times the stellar bolometric luminosity. The hard X-rays are also interpreted as lasting for timescales comparable with the flare soft X-ray emission, at variance with the Sun, where this nonthermal component, when present, is generally impulsive. Regardless of the true nature of the hard X-ray flux, the equivalent width measured from the II Peg *Swift* spectra ranges between 18 and 60 eV, corresponding to efficiency values $\mathcal{E}$ between 1% and 2%. These values are well within the range found from the theoretical calculations presented here and comparable with the measured value for HR 9024. Since the nonthermal hard X-ray component in the II Peg flare is not well constrained by the *Swift* data and could also be explained by thermal emission, the observed Fe Kα line seems more easily explained as arising from photoionization by flare X-rays (see also the discussion of D07b).

P. T. and D. P. H. were supported by SAO contract SV3-73016 to MIT for support of *CXC*, which is operated by SAO for and on behalf of NASA under contract NAS8-03060. J. J. D. was supported by the CXC NASA contract NAS8-39073. B. E. was supported by *Chandra* grants GO6-7008X and GO6-7098X. F. R., L. A., and G. M. acknowledge support from Agenzia Spaziale Italiana and Italian Ministero dell'Università e della Ricerca.

REFERENCES

Bai, T. 1979, Sol. Phys., 62, 113
Ballantyne, D. R., & Fabian, A. C. 2003, ApJ, 592, 1089
Bensby, T., Feltzing, S., & Lundström, I. 2003, A&A, 410, 527
Brickhouse, N. S., Dupree, A. K., & Young, P. R. 2001, ApJ, 562, L75
Canizares, C. R., et al. 2005, PASP, 117, 1144
Chung, S. M., Drake, J. J., Kashyap, V. L., Lin, L., & Ratzlaff, P. W. 2004, ApJ, 606, 1184
Culhane, J. L., et al. 1981, ApJ, 244, L141
Czesla, S., & Schmitt, J. H. H. M. 2007, A&A, 470, L13
Drake, J. J., & Ercolano, B. 2007, ApJ, 665, L175
Drake, J. J., Ercolano, B., & Swartz, D. A. 2007b, ApJ, in press (arXiv:0710:0621) (D07b)
Emslie, A. G., Phillips, K. J. H., & Dennis, B. R. 1986, Sol. Phys., 103, 89
Ercolano, B., Barlow, M. J., Storey, P. J., Liu, X.-W., Rauch, T., & Werner, K. 2003, MNRAS, 344, 1145
Ercolano, B., Young, P. R., Drake, J. J., & Raymond, J. C. 2007, ApJS, in press (arXiv:0710:2103)
Favata, F., Micela, G., Silva, B., Sciortino, S., & Tsujimoto, M. 2005, A&A, 433, 1047
Flaccomio, E., et al. 2005, ApJS, 160, 450
George, I. M., & Fabian, A. C. 1991, MNRAS, 249, 352
Giardino, G., Favata, F., Pillitteri, I., Flaccomio, E., Micela, G., & Sciortino, S. 2007, A&A, 475, 891
Houck, J. C., & Denicola, L. A. 2000, in ASP Conf. Ser. 216, Astron. Data Analysis Software and Systems IX, ed. N. Manset, C. Veillet, & D. Crabtree (San Francisco: ASP), 591
Huenemoerder, D. P., Testa, P., & Buzasi, D. L. 2006, ApJ, 650, 1119
Hussain, G. A. J., et al. 2005, ApJ, 621, 999
———. 2007, MNRAS, 377, 1488
Kashyap, V., & Drake, J. J. 2000, Bull. Astron. Soc. India, 28, 475
Marino, A., Micela, G., Peres, G., & Sciortino, S. 2003, A&A, 407, L63
Matranga, M., Mathioudakis, M., Kay, H. R. M., & Keenan, F. P. 2005, ApJ, 621, L125
Ness, J.-U., Güdel, M., Schmitt, J. H. M. M., Audard, M., & Telleschi, A. 2004, A&A, 427, 667
Osten, R. A., Drake, S., Tueller, J., Cummings, J., Perri, M., Moretti, A., & Covino, S. 2007, ApJ, 654, 1052
Parmar, A. N., Culhane, J. L., Rapley, C. G., Wolfson, C. J., Acton, L. W., Phillips, K. J. H., & Dennis, B. R. 1984, ApJ, 279, 866
Phillips, K. J. H., Pike, C. D., Lang, J., Watanbe, T., & Takahashi, M. 1994, ApJ, 435, 888
Reale, F., Güdel, M., Peres, G., & Audard, M. 2004, A&A, 416, 733
Reynolds, C. S., & Nowak, M. A. 2003, Phys. Rep., 377, 389
Singh, K. P., Drake, S. A., White, N. E., & Simon, T. 1996, AJ, 112, 221
Tanaka, K., Watanabe, T., & Nitta, N. 1984, ApJ, 282, 793
Testa, P., Drake, J., & Peres, G. 2004a, ApJ, 617, 508
Testa, P., Drake, J., Peres, G., & DeLuca, E. 2004b, ApJ, 609, L79
Testa, P., Drake, J. J., Peres, G., & Huenemoerder, D. P. 2007a, ApJ, 665, 1349
Testa, P., Reale, F., Garcia-Alvarez, D., & Huenemoerder, D. P. 2007b, ApJ, 663, 1232 (Paper I)
Tsujimoto, M., et al. 2005, ApJS, 160, 503
Vaiana, G. S., Davis, J. M., Giacconi, R., Krieger, A. S., Silk, J. K., Timothy, A. F., & Zombeck, M. 1973a, ApJ, 185, L47
Vaiana, G. S., Krieger, A. S., & Timothy, A. F. 1973b, Sol. Phys., 32, 81
White, N. E., Shafer, R. A., Parmar, A. N., Horne, K., & Culhane, J. L. 1990, ApJ, 350, 776
Zarro, D. M., Dennis, B. R., & Slater, G. L. 1992, ApJ, 391, 865